Published in Applied Physics Letters 75, 665-667, 1999
which should be used for any reference to this work


# Demonstration of high-performance 10.16 $\mu$m quantum cascade distributed feedback lasers fabricated without epitaxial regrowth

Daniel Hofstetter,[a] Jérôme Faist, Mattias Beck, and Antoine Müller
*University of Neuchâtel, Institute of Physics, 1 Rue A.-L. Breguet, Neuchâtel, CH 2000, Switzerland*

Ursula Oesterle
*Swiss Federal Institute of Technology Lausanne, Institute of Micro- and Optoelectronics, Physics Department, PHB Ecublens, CH 1015 Lausanne, Switzerland*

We present measurement results on high-power low threshold quantum cascade distributed feedback lasers emitting infrared radiation at 10.16 $\mu$m. A lateral current injection scheme allowed the use of a strongly coupled surface grating without metal coverage and epitaxial regrowth. Although this design resulted in a simplified processing, the fabrication of high performance devices was demonstrated. The laser emitted 230 mW of pulsed power at 85 K, and 80 mW at room temperature. Threshold current densities of 1.85 kA/cm$^2$ at 85 K and 5.4 kA/cm$^2$ at room temperature were observed. Since the spectrum showed single mode behavior for all temperatures and power levels of the operating range, this device will be ideal for optical sensor applications.

The development of high-performance midinfrared light sources has experienced tremendous progress during the last five years. Pacemakers of this progress were the appearance and the subsequent improvements of the quantum cascade (QC) laser.[1–3] For several potential applications, especially in the area of optical sensors for atmospheric trace gases, it is advantageous to operate with single mode, single frequency lasers. For this purpose, distributed feedback (DFB) QC lasers have been extensively investigated and characterized.[4–6] Although DFB lasers have obvious performance benefits, there are some severe fabrication drawbacks. One of them is the requirement of epitaxial regrowth, which makes fabrication rather complicated and prolonged. This is not only due to the regrowth process itself, but also because of the fact that the material can be tested only after grating fabrication and overgrowth.

A simple method to avoid epitaxial regrowth in DFB lasers consists of fabricating the grating directly on top of the waveguide.[4] However, in order to prevent the top contact metal from introducing a large waveguide loss (which is especially true for QC lasers operating in TM mode), one has to either decrease the grating coupling coefficient,[4] choose a metal with small refractive and absorption indices,[7] or completely avoid the metal on top of the waveguide.[8] The last possibility, which comes close to what we will describe in this article, was published under the name ''surface skimming'' laser. Such devices consist basically of a waveguide with a semiconductor lower cladding layer and air acting as top cladding. The heavily *n*-doped InGaAs cap layer, which serves as host layer for the grating, is highly conducting to allow lateral current injection and distribution throughout the device. The most important consequences of such a design are obviously that there is a large refractive index step between semiconductor and air, and that there are low calculated losses of 12 cm$^{-1}$. This results in both a high coupling coefficient of the grating and a relatively high net gain of the laser; thus it potentially allows the fabrication of short devices with a low threshold current.

Growth of this material was based on molecular beam epitaxy (MBE) of lattice matched InGaAs/InAlAs layers on top of an *n*-doped InP (Si, $2\times10^{17}$ cm$^{-3}$) substrate. The growth process started with the lower waveguide layers (InGaAs, Si, $1\times10^{17}$ cm$^{-3}$, total thickness 1.3 $\mu$m), proceeded with an active region (thickness 1.75 $\mu$m) and was finished by a thicker set of upper waveguide layers (thickness 2.1 $\mu$m) and a 0.5-$\mu$m-thick highly *n*-doped cap layer on top. This cap layer was also the host layer for the grating, as mentioned in the introduction. The active region, which thus formed the central part of the waveguide, consisted of 35 superlattice periods; those were alternating *n*-doped funnel injector regions and undoped triple quantum well active regions. The laser transition in the latter was diagonal, similar as described in Ref. 9. The layer sequence of the structure, in nanometers, starting from the injection barrier, is as follows: 3.9/**1.0**/3.8/**1.2**/3.7/**1.5**/3.9/**1.7**/4.0/**4.2**/3.1/**0.9**/6.4/**1.0**/6.0/**2.8** nm. $In_{0.52}Al_{0.48}As$ layers are in bold, $In_{0.53}Ga_{0.47}As$ layers are in roman, and *n*-doped layers (Si, $2.5\times10^{17}$ cm$^{-3}$) are underlined. A more detailed description of the layer thicknesses and compositions, as well as a schematic drawing of the band gap of one superlattice period including the relevant electronic transitions, will be published in a companion letter about wavelength tunable Fabry-Pérot lasers fabricated from material using the same active region.[10]

The fabrication of these DFB lasers was based on holographically defining a grating with 1.59 $\mu$m period ($n_{\text{eff}}=3.21$), and wet chemical etching of the grating in a $HBr:H_2O_2:H_2O$ solution to a depth of 0.4 $\mu$m. We used a 488 nm Ar-ion laser and a 90° corner reflector mounted on a rotational stage for the grating exposure. Standard processing

[a]Electronic mail: daniel.hofstetter@iph.unine.ch

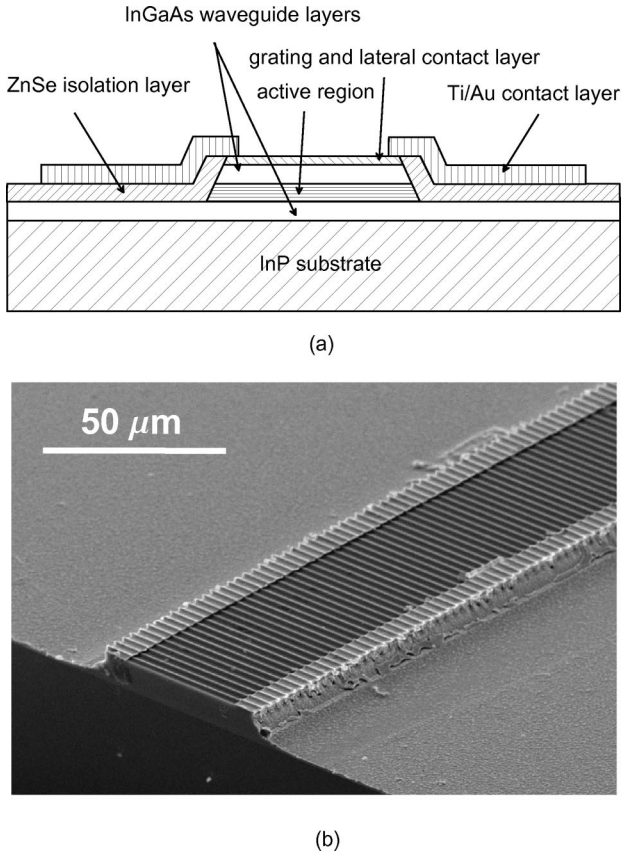


FIG. 1. (a) Schematic cross section through the laser waveguide showing the exact position of the grating with respect to the active layer and the metal top contact. (b) Scanning electron microscopy picture of a QC DFB laser. Please note that there is no metal in the central top part of the ridge waveguide.

techniques were then used to define ridge waveguides with a width of 35–55 $\mu$m (etch depth 4.5 $\mu$m) and a length of 1–1.5 mm.[3] 300 nm of ZnSe served as an electrical passivation layer and Ti/Au (10/400 nm) was used as top contact metal. Thinning, back contacting (Ge/Au/Ag/Au, 12/27/50/100 nm), and cleaving completed the processing. As shown by the schematic cross-section in Fig. 1(a) and the scanning electron microscopy picture in Fig. 1(b), the contact metal covered only the edges (about 5 $\mu$m on each side) of the ridge to prevent large absorption losses in the waveguide, but still allow lateral current injection. The devices, whose facets were left uncoated, were mounted ridge side up on copper heatsinks and operated at different temperatures between 85 and 300 K. The samples were then placed into a temperature controlled $N_2$ flow cryostat. The light of the QC DFB laser was collected by $f/0.8$ optics and fed into a high resolution Fourier transform spectrometer (Nicolet type Magna-IR 860), where we detected it using a liquid nitrogen-cooled HgCdTe detector. For the measurement of light–current ($L-I$) curves, we measured the intensity with a calibrated $500\times500\,\mu\text{m}^2$ room temperature HgCdTe detector. Typical $L-I$ and current–voltage ($I-V$) curves of a 45-$\mu$m-wide and 1.2-mm-long device are shown in Fig. 2. The current pulses were 100 ns long, and a pulse repetition frequency of 5 kHz was used for all temperatures. At low temperatures, we observed a threshold current of 1 A and a maximum output power of 230 mW for 9.7 V bias voltage. The slope efficiency at this temperature was 220 mW/A and a threshold

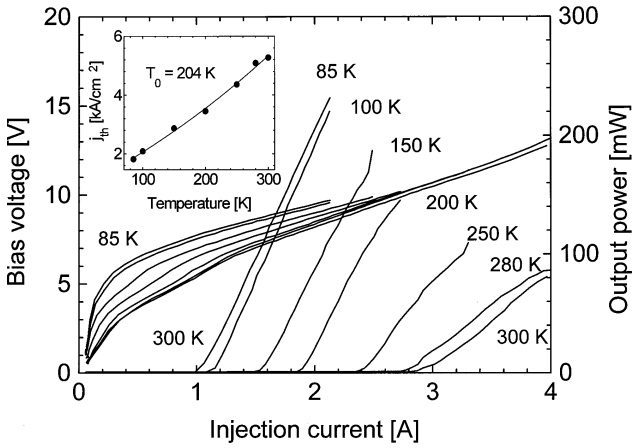


FIG. 2. $L-I$ and $I-V$ curves of a 45-$\mu$m-wide and 1.2-mm-long DFB QC laser measured at different temperatures. The inset shows a plot of the threshold current vs device temperature.

current density of 1.85 kA/cm$^2$ was determined. At room temperature, we still obtained 80 mW optical output power with a slope efficiency of 80 mW/A; however, the threshold current increased to 2.9 (threshold current density of 5.4 kA/cm$^2$), and an operating voltage of 12.5 V was seen. From the increase in threshold current, we were able to derive a characteristic temperature $T_0$ of 204 K.

In Fig. 3, we present three luminescence spectra measured at 85, 105, and 150 K. In all of them, the spontaneous emission peaks around 980 cm$^{-1}$, and there occur regular Fabry–Pérot modes with a spacing of 1.7 cm$^{-1}$ (cavity length: 850 $\mu$m). The Bragg reflector's stop band with a width of 2.5 cm$^{-1}$ is clearly visible at 995.7 (85 K), 994.6 (105 K), and 992.3 cm$^{-1}$ (150 K). From the stop bandwidth, we determined the coupling coefficient of the grating to be $\kappa=\Delta\lambda\,\pi n_{\text{eff}}/\lambda^2=24\,\text{cm}^{-1}$; this number agrees well with a value obtained from an estimation based on the effective refractive index difference of $\Delta n=1.8\times10^{-2}$ between areas with and without the grating layer ($\kappa=\pi\Delta n_{\text{eff}}/2\lambda=28\,\text{cm}^{-1}$). A relatively small free carrier absorption loss of 12 cm$^{-1}$ was calculated for this device, whereas a laser utilizing our standard waveguide design with a 2.2-$\mu$m-thick InAlAs/InGaAs upper cladding layer and a metal-covered

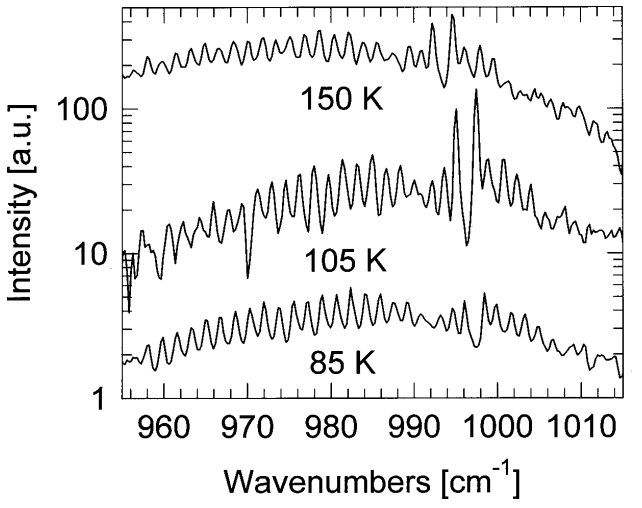


FIG. 3. Spontaneous emission spectra of a 45-$\mu$m-wide and 850-$\mu$m-long DFB QC laser at 85, 105, and 150 K.

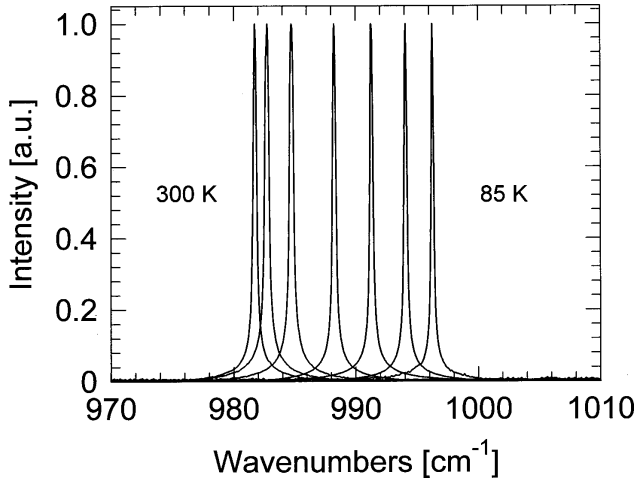


FIG. 4. Lasing spectra of a 45-$\mu$m-wide and 1.2-mm-long DFB QC laser at different temperatures between 85 and 300 K. All spectra were measured with the maximum possible output power at each individual temperature.

grating would suffer from a waveguide loss of 30 $cm^{-1}$. In addition, the refractive index contrast would be reduced by almost two orders of magnitude, namely to a value of $\Delta n = 2.3\times10^{-4}$. Since the partial removal of the contact layer leads to a slight gain variation, a small amount of loss coupling might also be present in this device.

Figure 4 shows the lasing spectra at temperatures between 85 and 300 K. We observed single mode operation for all temperatures and, in particular, at maximum power for each individual temperature. We determined the linewidth to be on the order of 0.3 $cm^{-1}$, which corresponds to the resolution limit of our experimental setup. The emission wavelength at 85 K was 996 $cm^{-1}$; at room temperature, it decreased to 982 $cm^{-1}$. As already mentioned above, the luminescence peak was found in the vicinity of 975 $cm^{-1}$ for all temperatures. The temperature tuning coefficient of the lasing peak was constant over the entire temperature range, and its magnitude was $1/\lambda\times\Delta\lambda/\Delta T = 6.5\times10^{-5}\,K^{-1}$ ($\Delta\nu/\Delta T = -0.063\,cm^{-1}/K$). These numbers are consistent with what has been reported in the literature.[5]

By utilizing a second processing run with a changed grating period of 1.63 $\mu$m (instead of 1.59 $\mu$m), we were able to perform some measurements regarding the influence of a detuning between Bragg peak and gain peak. The first series of DFB lasers with a detuning of about 5–10 $cm^{-1}$ at room temperature ($\Lambda = 1.59\,\mu m$) showed high performance at all temperatures. The second series with a detuning of about 30 $cm^{-1}$ ($\Lambda = 1.63\,\mu m$) did not lase at room temperature, and at low temperatures, the output power did not exceed 60 mW. Since we determined a full width at half maximum (FWHM) of the gain peak of $\Delta\nu = 65\,cm^{-1}$, it is clear that the laser performance will degrade rapidly with increasing detuning between Bragg reflection maximum and gain peak.

In conclusion, we have shown device results for a DFB QC laser operating at 10.16 $\mu$m. This DFB laser functions without upper cladding layer; the grating is therefore directly exposed to air. Current injection is accomplished laterally through the grating layer; this design avoids large waveguide losses due to metal absorption. Although the fabrication of this device is straightforward, without epitaxial regrowth, we achieved a very good performance. At room temperature, the laser emitted 80 mW optical power at single mode operation. Pulsed threshold current densities of 5.4 and 1.85 $kA/cm^{-2}$, and slope efficiencies of 220 and 80 mW/A at 85 and 300 K, respectively, were obtained. This device will have important applications in optical sensing of ammonia and other atmospheric trace gases.

We would like to thank Thierry Aellen, Stéphane Blaser, and Michel Rochat for their advice during processing, electrical, and spectral measurements on these samples, Hans-Peter Herzig, Philippe Nussbaum, and René Dändliker from the Institute for Microtechnology at the University of Neuchâtel for their support in grating fabrication, and the Swiss National Science foundation and the Science Foundation of the European community for their financial support (project UNISEL, BRITE/EURAM, No. CT97-0557).

[1] J. Faist, F. Capasso, D. L. Sivco, A. L. Hutchinson, and A. Y. Cho, Science **264**, 553 (1994).
[2] J. Faist, F. Capasso, C. Sirtori, D. L. Sivco, J. N. Baillargeon, A. L. Hutchinson, S. N. G. Cho, and A. Y. Cho, Appl. Phys. Lett. **68**, 3680 (1996).
[3] C. Sirtori, J. Faist, F. Capasso, D. L. Sivco, A. L. Hutchinson, and A. Y. Cho, Appl. Phys. Lett. **68**, 1745 (1996).
[4] J. Faist, C. Gmachl, F. Capasso, C. Sirtori, D. L. Sivco, J. N. Baillargeon, and A. Y. Cho, Appl. Phys. Lett. **70**, 2670 (1997).
[5] C. Gmachl, J. Faist, J. N. Baillargeon, F. Capasso, C. Sirtori, D. L. Sivco, S. N. G. Chu, and A. Y. Cho, IEEE Photonics Technol. Lett. **9**, 1090 (1997).
[6] C. Gmachl, F. Capasso, J. Faist, A. L. Hutchinson, A. Tredicucci, D. L. Sivco, J. N. Baillargeon, S. N. G. Chu, and A. Y. Cho, Appl. Phys. Lett. **72**, 1430 (1998).
[7] C. H. Wu, P. S. Zory, and M. A. Emanuel, IEEE Photonics Technol. Lett. **6**, 1427 (1994).
[8] R. L. Thornton, W. J. Mosby, and H. F. Chung, Appl. Phys. Lett. **59**, 513 (1991).
[9] J. Faist, C. Sirtori, F. Capasso, D. L. Sivco, J. N. Baillargeon, A. L. Hutchinson, and A. Y. Cho, IEEE Photonics Technol. Lett. **10**, 1100 (1998).
[10] A. Müller, M. Beck, and J. Faist, Appl. Phys. Lett. (to be published).